

1 Synthesis and characteristics of organotin-based catalysts for acetylene 2 hydrochlorination

3 Yi-BoWu¹, Bo-WenLi¹, Fu-XiangLi¹, Jian-WeiXue¹, Zhi-Ping Lv¹

4 ¹Research Institute of Special Chemicals, Taiyuan University of technology, Taiyuan,
5 030024, P. R. China.

6 **Corresponding author:** Fu-Xiang Li, e-mail: L63f64x@163.com .

7 Abstract

8 Organotin-based catalysts prepared by a facile and green synthesis route were used in
9 the acetylene hydrochlorination reaction. In detail, organotin-based catalysts were directly
10 synthesized by supporting both organotin and nitrogen compounds on a coal-based columnar
11 activated carbon (AC) using both incipient wetness impregnation and calcination methods.
12 Interestingly, upon addition of nitrogen compounds, the resultant (SnCl₄+C₁₆H₃₄Cl₂Sn)/AC
13 catalysts showed higher activity and stability when compared to its
14 (SnCl₄+C₁₆H₃₄Cl₂Sn+C₂N₄H₄)/AC counterpart at 200 °C and a gas hourly space velocity
15 (GHSV, C₂H₂ based) of 30 h⁻¹. According to the results, organotin was demonstrated to be the
16 active site, while the incorporation of nitrogen allowed to partly mitigate the loss of active
17 components.

18 **Keywords:** organotin-based catalyst; organotin compounds; nitrogen compounds; acetylene
19 hydrochlorination.

20 1. Introduction

21 Polyvinylchloride (PVC) plays a significant role in agriculture, industry, electronic
22 science and national defense.¹ The industrial production of PVC is typically carried out by
23 direct chlorination of ethylene, oxychlorination of ethylene, and acetylene hydrochlorination,
24 the latter of which is widely used in coal-rich regions of China.² Nevertheless, the traditional
25 mercury-based catalysts used to carry out this reaction are easily lost during the course of the

26 reaction. Additionally, mercuric chloride constitutes a potential threat to the environment and
27 to the human health. Thus, developing non-mercury catalysts represents a sustainable
28 acetylene production route.

29 Hutchings et al. reported Au-based catalysts to have superior catalytic performance
30 towards the hydrochlorination of acetylene and studied in detail the reaction mechanism of
31 these materials. The reduction of Au³⁺ was associated with catalyst deactivation.^{1,3,4} Although
32 precious-metal catalysts show excellent catalytic performance, it is of great significance to
33 explore non-precious metal catalysts with reduced cost. With this aim, numerous researchers
34 have started to develop new-type catalysts.⁵⁻¹³ Later, Dai et al prepared boron-and nitrogen-
35 doped graphene catalysts that displayed superior catalytic activity towards acetylene
36 hydrochlorination and demonstrated that boron and nitrogen can promote hydrogen chloride
37 adsorption.⁷ Additionally, the Dai's group also reported AC-supported transition metal
38 nitrides to show better activity and selectivity towards acetylene hydrochlorination.¹¹

39 In the past few years, tin compounds have been investigated as promoters to reduce
40 coke deposition and therefore improve the catalytic activity and the stability of catalysts.¹⁴⁻¹⁷
41 Moreover, numerous diorganotins and triorganotins have been widely used as stabilizers,
42 catalysts and treatment materials for industrial and agricultural applications owing to their
43 unique structure, low toxicity and superior activity.¹⁸⁻²² In addition, Shinoda found that the
44 hydrochlorination activities of metal chlorides correlate with the affinity of the metal cation,
45 although their study did not include tin ions.²³ Moreover, Zhang et al. reported that the
46 superior catalytic performance and relatively long lifetime of Au-Sn/AC catalysts can be
47 improved by adding SnCl₂·2H₂O, which prevented coke deposition.⁸ At the same time,
48 organotin has been scarcely studied as an active site for the hydrochlorination of acetylene.
49 Having this in mind, the better activity of organotin motivated us to prepare organotin-based
50 materials were applied in acetylene hydrochlorination.

51 In this article, we successfully synthesized organotin-based catalysts using highly
52 porous AC as a support. We simultaneously carried out thermogravimetry/differential thermal
53 analysis (TG-DTA), scanning electron microscopy coupled with energy dispersive X-ray
54 spectrometry (SEM-EDS) elemental mapping and low-temperature nitrogen
55 adsorption/desorption experiments to characterize the organotin-based catalyst.

56 2. Experimental

57 2.1 Catalyst preparation

58 The raw material (a coal-based columnar AC) was pre-treated with HCl (0.01 mol/L)
59 to remove impurities, thoroughly washed with distilled water until neutral pH, and finally
60 dried at 120 °C for 24 h.

61 The organotin-based catalyst was synthesized by an incipient wetness impregnation
62 technique using AC as a support. The impregnating solution was prepared by dissolving
63 dioctyldichlorotin (2.0 g) and tin (IV) chloride (2.0 g) in ethanol (100 mL) in a beaker. The
64 solution was stirred at 80 °C (water bath) for 30 min. Subsequently, 16 g of fresh AC were
65 gradually added under stirring, and the resulting mixture was stirred at 80 °C for 2 h and
66 finally dried in an oven at 100 °C for 12 h. The product was heated to 200 °C under flowing
67 nitrogen for 4 h with a heating rate of 10 °C/min to finally yield the catalyst. In addition,
68 different samples were prepared by the same method for comparison. 20%
69 (SnCl₄+C₁₆H₃₄Cl₂Sn)/AC-200 indicates that the dioctyldichlorotin and tin (IV) chloride
70 loading in all the catalysts was fixed at 20 wt% and the calcination temperature was 200 °C.

71 2.2 Catalytic performance tests

72 The performance of the organotin-based catalyst was determined in a fix-bed glass
73 reactor (i.d. =10mm) at atmospheric pressure. Before initiating the reaction, hydrogen chloride
74 was passed through the fix-bed to remove air and water from the reaction system (60min).
75 Once the reactor reached the desired temperature (150–200 °C), the gas mixture (HCl/C₂H₂

76 =1.1:1.0) was calibrated using mass flowmeters and fed into the reactor containing 3.2 mL of
77 catalyst (gas hourly space velocity (GHSV) of 30 h⁻¹). The outlet gas was passed through a
78 glass tube containing medical soda-lime to absorb the unreacted HCl and immediately
79 analyzed on-line using a gas chromatograph (GC900) equipped with a GDX-301 column.

80 2.3 Catalyst characterization

81 The Brunauer–Emmett–Teller (BET) surface area and pore volume of the samples
82 were measured by nitrogen adsorption at 77 K using a Quantachrome Nova 2000e gas
83 sorption analyser. All the catalysts were degassed at 100 °C for 5h before the analysis.

84 The weight loss and stability of the catalysts were analyzed by TG-DTA (NETZSCH
85 STA 449F3) under a nitrogen flow of 30 mL/min and at a heating rate of 30 °C/min within a
86 temperature range of 25–800 °C.

87 The SEM micrographs and the EDS elemental maps were recorded on a TEACAN
88 MAIA3 microscope at an acceleration voltage of 15 kV.

89 3. Results and discussion

90 3.1 Catalytic performance

91 The surface area and pore volume of the different samples are listed in Table 1, while the
92 catalytic performance of the catalysts is shown in Fig. 1. Fresh AC shows a negligible
93 conversion despite showing the highest specific surface area (987.2 m²/g). Upon calcination at
94 higher temperature, the specific surface area and micropore volume of the 20% C₂N₄H₄/AC-
95 550 sample decreased to 577.9 m²/g and 0.30 cm³/g, respectively, while the maximum
96 acetylene conversion reached 22.5%. Owing to dicyandiamide is easily transformed into g-
97 C₃N₄,²⁵ which was mostly dispersed on the micropores of the carbon material improving the
98 acetylene conversion. Interestingly, 20% C₁₆H₃₄Cl₂Sn/AC-200 significantly increased its
99 catalytic activity at 200 °C and showed higher activity than SnCl₄/AC-200. This result, along

100 with data in Table 1, confirmed that organotin was successfully loaded on AC and played an
101 active site in the acetylene hydrochlorination reaction.

102 Fig. 1b shows the effect of the dioctyldichlorotin loading (5-25wt%) on the catalytic
103 performance. The acetylene conversion gradually increased (from 36.3 to 86.4%) with the
104 dioctyldichlorotin loading increasing from 5 to 25 wt%. The decrease in surface area and pore
105 volume with the dioctyldichlorotin loading can be attributed to dioctyldichlorotin partly
106 blocking the surface of the support. 20% $C_{16}H_{34}Cl_2Sn/AC$ shows higher acetylene
107 conversions than 25% $C_{16}H_{34}Cl_2Sn/AC$. Thus, the catalytic activity increased with the
108 dioctyldichlorotin content up to 20 wt%.

109 Because of the activity of dioctyldichlorotin and tin (IV) chloride, we focused our
110 investigations on the catalyst containing both components (i.e., $(SnCl_4+C_{16}H_{34}Cl_2Sn)/AC$)
111 which showed better catalytic performance than $C_{16}H_{34}Cl_2Sn/AC$ and $SnCl_4/AC$. Importantly,
112 the mixture of dioctyldichlorotin and tin (IV) chloride can effectively reduce the cost of the
113 organotin-based catalysts.

114 3.2 Catalytic performance of $(SnCl_4+C_{16}H_{34}Cl_2Sn)/AC$

115 The Kocheshkov redistribution reaction is commonly carried out without solvent and
116 thus it was necessary to investigate the effect of the calcination temperature and mole ratio of
117 tin compounds on the catalytic performance of the materials prepared.²⁶ As shown in Table 2,
118 the external surface area of $(SnCl_4+C_{16}H_{34}Cl_2Sn)/AC$ gradually increased with the calcination
119 temperature, indicating that dioctyldichlorotin reacted with tin (IV) chloride at an optimal
120 calcination temperature of 200 °C. As depicted in Fig. 2a, the optimum catalytic activity of
121 $(SnCl_4+C_{16}H_{34}Cl_2Sn)/AC-200$ was not ascribed to its specific surface and volume
122 characteristics. Instead, the nature of the active site has a significant influence on the
123 acetylene conversion. As shown in Fig. 2b, the $SnCl_4:C_{16}H_{34}Cl_2Sn$ mole ratio was 1.6:1.0,
124 suggesting that tin (IV) chloride reacted with dioctyldichlorotin to generate octyltrichlorotin.

125 This was further supported by the fact that tin (IV) chloride was easily volatilized at
126 temperatures lower than the reaction temperature (114.5 °C). As illustrated in Fig. 2a, the
127 maximum acetylene conversion of (SnCl₄+C₁₆H₃₄Cl₂Sn)/AC-200 was 89.1% at 200 °C, at a
128 SnCl₄:C₁₆H₃₄Cl₂Sn mole ratio of 1.6:1.0. However, this catalyst showed the maximum weight
129 loss rate at 230.6 °C (Fig. 5), and we tried to improve the stability of the catalyst by adding
130 some components. For instance, Zhang et al. developed a nitrogen-modified carbon supported
131 AuCl₃ catalyst with superior stability, which was ascribed to nitrogen inhibiting the Au³⁺ to
132 Au⁰ reaction and enhancing the adsorption of hydrogen chloride.²⁷ By temperature-
133 programmed adsorption and density functional theory (DFT) calculations, Dai et al. revealed
134 that the addition of nitrogen can improve the adsorption of HCl.⁶ Therefore, we used
135 dicyandiamide as a precursor of g-C₃N₄ for improving the lifetime of the
136 (SnCl₄+C₁₆H₃₄Cl₂Sn)/AC catalyst.

137 3.3 Catalytic performance of (SnCl₄+C₁₆H₃₄Cl₂Sn+C₂N₄H₄)/AC

138 As shown in Table 3, the specific surface area and total pore volume of
139 (SnCl₄+C₁₆H₃₄Cl₂Sn+C₂N₄H₄)/AC were slightly higher than that of
140 (C₁₆H₃₄Cl₂Sn+SnCl₄)/AC prepared at similar synthesis conditions, indicating that the active
141 compounds were successfully loaded on the support. In addition, the catalytic performance
142 of (SnCl₄+C₁₆H₃₄Cl₂Sn+C₂N₄H₄)/AC (Fig. 2a and 3a) and (SnCl₄+C₁₆H₃₄Cl₂Sn)/AC
143 indistinctively changed over the temperature range of 150 - 300 °C, showing that nitrogen
144 compounds played a small effect on the acetylene conversion of organotin-based catalysts
145 at lower calcination temperatures. Over the temperature range of 350-500 °C (Fig. 3b),
146 (SnCl₄+C₁₆H₃₄Cl₂Sn+C₂N₄H₄)/AC-400 shows the lowest specific surface and total volume
147 values among the samples studied (233.0 m²/g and 0.15 cm³/g, respectively), indicating that
148 dicyandiamide may have reacted with tin (IV) chloride and dioctyldichlorotin to produce
149 molecules with larger molecular weight. Therefore, it is essential to study in detail the

150 effect of the calcination temperature or nitrogen compounds on the conversion of acetylene.
151 As shown in Fig. 3c, $(\text{SnCl}_4+\text{C}_{16}\text{H}_{34}\text{Cl}_2\text{Sn}+\text{C}_2\text{N}_4\text{H}_4)/\text{AC}$ -400 showed the best performance
152 among the organotin samples with an acetylene conversion of 92.1%. Thus, the optimal
153 calcination temperature of $(\text{SnCl}_4+\text{C}_{16}\text{H}_{34}\text{Cl}_2\text{Sn}+\text{C}_2\text{N}_4\text{H}_4)/\text{AC}$ was 400 °C. The external
154 surface seems to influence the catalytic performance to a larger extent as compared to the
155 micropore surface (Table 3). With regard to the nitrogen-doped catalysts,
156 $(\text{SnCl}_4+\text{C}_{16}\text{H}_{34}\text{Cl}_2\text{Sn}+\text{C}_2\text{N}_4\text{H}_4)/\text{AC}$ -400 showed slightly higher acetylene conversions than
157 that of $(\text{SnCl}_4+\text{C}_{16}\text{H}_{34}\text{Cl}_2\text{Sn})/\text{AC}$ -200 and $(\text{SnCl}_4+\text{C}_{16}\text{H}_{34}\text{Cl}_2\text{Sn})/\text{AC}$ -400, illustrating that
158 the addition of nitrogen has a positive effect on the acetylene conversion at higher
159 calcination temperature, in line with results shown in Fig. 4a. The stability of both
160 catalysts should be investigated in detail.

161 3.4 Stability of $(\text{SnCl}_4+\text{C}_{16}\text{H}_{34}\text{Cl}_2\text{Sn})/\text{AC}$ and $(\text{SnCl}_4+\text{C}_{16}\text{H}_{34}\text{Cl}_2\text{Sn}+\text{C}_2\text{N}_4\text{H}_4)/\text{AC}$

162 The catalytic performance and stability of $(\text{SnCl}_4+\text{C}_{16}\text{H}_{34}\text{Cl}_2\text{Sn}+\text{C}_2\text{N}_4\text{H}_4)/\text{AC}$ and
163 $(\text{SnCl}_4+\text{C}_{16}\text{H}_{34}\text{Cl}_2\text{Sn})/\text{AC}$ are illustrated in Fig. 4. By thermal condensation experiments, the
164 addition of dicyandiamide showed a minimal effect on the catalytic activity and selectivity,
165 whereas it dramatically improved the stability of the catalysts. As shown in Fig. 4a,
166 $(\text{SnCl}_4+\text{C}_{16}\text{H}_{34}\text{Cl}_2\text{Sn}+\text{C}_2\text{N}_4\text{H}_4)/\text{AC}$ showed higher catalytic activity and longer lifetimes than
167 $(\text{SnCl}_4+\text{C}_{16}\text{H}_{34}\text{Cl}_2\text{Sn})/\text{AC}$ (92.1 versus 72.1% acetylene conversion) after 36 h on stream. The
168 acetylene conversion of $(\text{SnCl}_4+\text{C}_{16}\text{H}_{34}\text{Cl}_2\text{Sn})/\text{AC}$ decreased from 89.1 to 49.5% after 36 h on
169 stream, revealing poor stability towards the acetylene hydrochlorination reaction. As shown in
170 Fig. 4b, the selectivity towards vinyl chloride monomer (VCM) was above 97.5%. This result
171 demonstrated that organotin are highly active and selective species, while the addition of
172 dicyandiamide can strengthen the catalytic stability of organotin-based catalysts during the
173 hydrochlorination of acetylene. While the catalytic performance of the organotin-based

174 catalysts was slightly poorer than that of 10% HgCl_2/AC , the organotin-based catalysts
175 showed a better selectivity towards vinyl chloride.

176 The TGA results (Fig. 5) confirmed that the addition of dicyandiamide is the main
177 factor affecting the catalytic stability. $(\text{SnCl}_4+\text{C}_{16}\text{H}_{34}\text{Cl}_2\text{Sn})/\text{AC}$ showed a mass loss of 22.7%,
178 in agreement with the loaded amount of active component. Nevertheless,
179 $(\text{SnCl}_4+\text{C}_{16}\text{H}_{34}\text{Cl}_2\text{Sn}+\text{C}_2\text{N}_4\text{H}_4)/\text{AC}$ showed a mass loss close to 13.7%, while the maximum
180 weight loss rates of the $\text{SnCl}_4+\text{C}_{16}\text{H}_{34}\text{Cl}_2\text{Sn})/\text{AC}$ and $(\text{SnCl}_4+\text{C}_{16}\text{H}_{34}\text{Cl}_2\text{Sn}+\text{C}_2\text{N}_4\text{H}_4)/\text{AC}$
181 samples were found at 298.9 and 230.6 °C, respectively. Fig. 5 and 6 confirmed that
182 dicyandiamide was added to organotin via calcination, being transformed into a novel
183 compound with a reduced maximum weight loss temperature.

184 We selected several areas to investigate the dispersion of tin and chlorine on the fresh
185 and used catalysts via EDS elemental mapping. As shown in Fig. 6a and c, tin and chlorine
186 were highly dispersed on the surface of the fresh- $(\text{SnCl}_4+\text{C}_{16}\text{H}_{34}\text{Cl}_2\text{Sn})/\text{AC}$ and fresh-
187 $(\text{SnCl}_4+\text{C}_{16}\text{H}_{34}\text{Cl}_2\text{Sn}+\text{C}_2\text{N}_4\text{H}_4)/\text{AC}$ samples. The distribution of tin in the used-
188 $(\text{SnCl}_4+\text{C}_{16}\text{H}_{34}\text{Cl}_2\text{Sn})/\text{AC}$ and used- $(\text{SnCl}_4+\text{C}_{16}\text{H}_{34}\text{Cl}_2\text{Sn}+\text{C}_2\text{N}_4\text{H}_4)/\text{AC}$ samples is shown in
189 Fig. 6b and d. The results of Fig. 5 and 6a and 6c strongly confirmed that organotin was
190 successfully loaded on the coal-based columnar AC. Table 4 indicated that a large amount of
191 tin was dispersed on the surface of used- $(\text{SnCl}_4+\text{C}_{16}\text{H}_{34}\text{Cl}_2\text{Sn}+\text{C}_2\text{N}_4\text{H}_4)/\text{AC}$ versus used-
192 $(\text{SnCl}_4+\text{C}_{16}\text{H}_{34}\text{Cl}_2\text{Sn})/\text{AC}$, because the incorporation of nitrogen effectively and significantly
193 reduced the loss of tin during reaction. Combining the above results, it is concluded that
194 organotin acted as a catalytic active site and the incorporation of nitrogen strongly enhanced
195 the stability of organotin-based catalysts.

196 4. Conclusion

197 In this paper, we successfully synthesized organotin-based catalysts having superior
198 catalytic performance and stability towards the hydrochlorination of acetylene. These

199 catalysts were prepared by loading organotin and nitrogen compounds on an AC under
200 optimal conditions. The characterization data demonstrated that the effective addition of
201 dicyandiamide can prolong the lifetime of the organotin-based catalysts, and organotin played
202 a positive effect in increasing the acetylene conversion.

203 References

- 204 (1) Johnston, P.; Carthey, N.; Hutchings, G.J. *Journal of the American Chemical*
205 *Society*. 2015, 137, 14548
- 206 (2) Lin, R.; Amrute, A.P.; Perez-Ramirez, J. *Chemical Reviews*. 2017, 117, 4182
- 207 (3) Malta, G.; Kondrat, S.A.; Freakley, S.J.; Davies, C.J.; Lu, L.; Dawson, S.; Thetford, A.;
208 Gibson, E.K.; Morgan, D.J.; Jones, W.; Wells, P.P.; Johnston, P.; Catlow, C.R.A.; Kiely,
209 C.J.; Hutchings, G.J. *Science*. 2017, 355,1399
- 210 (4) Conte, M.; Carley, A.F.; Heirene, C.; Willock, D.J.; Johnston, P.; Herzing, A.A.;
211 Hutchings, G.J. *Journal of catalysis*. 2007, 250, 231
- 212 (5) Zhou, K.; Wang, W.; Zhao, Z.; Luo, G.; Miller, J.T.; Wong, M.;Wei, F. *ACS Catalysis*.
213 2014, 4, 3112
- 214 (6) Dai, B.; Chen, K.; Wang, Y.; Kang, L.; Zhu, M. *ACS Catalysis*. 2015, 5, 2541
- 215 (7) Dai,H.; Zhu, M.; Zhang, H.; Yu, F.; Wang, C.; Dai, B. *Journal of Industrial and*
216 *Engineering Chemistry*. 2017, 50, 72
- 217 (8) Dong, Y.; Zhang, H.; Li, W.; Sun, M.; Guo, C.; Zhang, J. *Journal of Industrial and*
218 *Engineering Chemistry*. 2016, 35, 177
- 219 (9) Pu,Y.; Zhang, J.; Wang,X.; Zhang, H.; Yu, L.; Dong, Y.; Li, W. *Catalysis Science &*
220 *Technology*. 2014, 4, 4426
- 221 (10) Wang, S.; Shen, B.; Song, L.Q. *Catalysis letters*. 2010, 134, 102
- 222 (11) Xu, N.; Zhu, M.; Zhang, J.; Zhang, H.; Dai, B. *RSC Advances*. 2015, 5, 86172

- 223 (12) Zhang, H.; Dai, B.; Wang, X.; Xu, L.; Zhu, M. *Journal of Industrial and Engineering*
224 *Chemistry*. 2012, 18, 49
- 225 (13) Jiang, L.; Sun, G.; Sun, S.; Liu, J.; Tang, S.; Li, H.; Xin,
226 Q. *ElectrochimicaActa*. 2005, 50,5384
- 227 (14) Kappenstein, C.; Gue, M.; Lázár, K.; Matusek, K.; Paál, Z. *Journal of the Chemical*
228 *Society. Faraday Transactions*. 1998, 94, 2463
- 229 (15) López-Suárez, F.E.; Bueno-López, A.; Eguiluz, K.I.B.; Salazar-Banda, G.R. *Journal of*
230 *Power Sources*. 2014, 268, 225
- 231 (16) Paál, Z.; Gyóry, A.; Uszkurat, I.; Olivier, S.; Guérin, M.; Kappenstein, C. *Journal of*
232 *Catalysis*. 1997, 168,164
- 233 (17) Zhang, S.; Duan, X.; Ye, L.; Lin, H.; Xie, Z.;Yuan,Y. *Catalysis today*. 2013, 215, 260
- 234 (18) Zhao, J.; Xu, J.; Xu, J.; Ni, J.; Zhang, T.; Xu, X.; Li, X. *ChemPlusChem*. 2015, 80,
235 196
- 236 (19) Bulatović, M.Z.; Maksimović-Ivani, D.; Bensing, C.; Gómez-Ruiz, S.; Steinborn, D.;
237 Schmidt, H.; Mojić, M.; Korac, A.; Golic, I.; Pérez-Quintanilla, D.; Momčilović, M.;
238 Mijatovic,S.; Mijatovic, G.N. *Angewandte Chemie International Edition*. 2014, 53, 5982
- 239 (20) Byrd, J.T.; Andrae, M.O. *Science*. 1982, 218, 565
- 240 (21) Shah, M.; Ali, S.; Tariq, M.; Khalid, N.; Ahmad, F.; Khan, M.A. *Fuel*. 2014, 118, 392
- 241 (22) Starnes, W.H.; Plitz, I.M. *Macromolecules*. 1976, 9, 633
- 242 (23) Shinoda, K. *Chemistry letters*. 1975, 4, 219
- 243 (24) Suzuki, T.; Ando, T.; Yamada, O.; Watanabe, Y. *Fuel*. 1986, 65, 786
- 244 (25) Thomas, A.; Fischer, A.; Goettmann, F.; Antonietti, M.; Müller, J.O.; Schlögl, R.;
245 Carlsson, J. M. *Journal of Materials Chemistry*. 2008, 18, 4893
- 246 (26) Ingham, R.K.; Rosenberg, S.D.; Gilman, H. *Chemical reviews*. 1960, 60,459

247 (27) Gu, J.; Du, Q.; Han, Y.; He, Z.; Li, W.; Zhang, J. *Physical Chemistry Chemical*
248 *Physics*. 2008, 18, 4893

249

250

251

252

253

254

255

256

257

258

259

260

261

262

263

264

265

266

267

268

269

270

271

Tables

272

273 **Table 1.** Textural properties of the different catalysts.

274 [a] S_{BET} is the surface area calculated using the Brunauer–Emmett–Teller (BET) equation

275 over the relative pressure range of 0.05–0.03. [b] Micropore surface area. [c] External surface

276 area calculated by the t-plot method. [d] $V_{\text{meso}} = V_{\text{total}} - V_{\text{mic}}$ (V_{mic} , micropore volume) is also

277 calculated by the t-plot method. [e] V_{total} (total volume) at $P/P_0=0.99$ is derived from the

278 nitrogen adsorption isotherm.

279

Sample	Calcinations Temperature (°C)	S_{BET} (m^2/g) ^a	S_{mic} (m^2/g) ^b	S_{ext} (m^2/g) ^c	V_{mic} (m^3/g)	V_{meso} (m^3/g) ^d	V_{total} (m^3/g) ^e
AC-200	200	987.2	864.5	122.7	0.12	0.36	0.48
20% $\text{C}_2\text{N}_4\text{H}_4/\text{AC}$ -550	550	641.9	577.9	64.0	0.23	0.07	0.30
20% SnCl_4/AC -200	200	474.2	422.6	51.6	0.18	0.05	0.23
25% $\text{C}_{16}\text{H}_{34}\text{Cl}_2\text{Sn}/\text{AC}$ -200	200	84.7	51.4	33.8	0.06	0.02	0.08
20% $\text{C}_{16}\text{H}_{34}\text{Cl}_2\text{Sn}/\text{AC}$ -200	200	156.4	122.3	34.1	0.06	0.03	0.09
15% $\text{C}_{16}\text{H}_{34}\text{Cl}_2\text{Sn}/\text{AC}$ -200	200	281.8	223.4	58.4	0.10	0.06	0.16
10% $\text{C}_{16}\text{H}_{34}\text{Cl}_2\text{Sn}/\text{AC}$ -200	200	408.9	335.6	73.3	0.14	0.07	0.21
5% $\text{C}_{16}\text{H}_{34}\text{Cl}_2\text{Sn}/\text{AC}$ -200	200	523.2	450.3	72.9	0.19	0.07	0.26

280

281

282

283

284

285

286

287

288

289 **Table 2.** Textural properties of (SnCl₄+C₁₆H₃₄Cl₂Sn)/AC at different calcination
 290 temperatures. The molar ratio of SnCl₄ and C₁₆H₃₄Cl₂Sn was 1.6:1.0.

291

Sample	Calcinations Temperature (°C)	S _{BET} (m ² /g) ^a	S _{mic} (m ² /g) ^b	S _{ext} (m ² /g) ^c	V _{mic} (m ³ /g)	V _{meso} (m ³ /g) ^d	V _{total} (m ³ /g) ^e
(SnCl ₄ +C ₁₆ H ₃₄ Cl ₂ Sn)/AC-150	150	442.6	237.2	205.4	0.13	0.11	0.24
(SnCl ₄ +C ₁₆ H ₃₄ Cl ₂ Sn)/AC-200	200	243.5	143.0	100.5	0.11	0.04	0.15
(SnCl ₄ +C ₁₆ H ₃₄ Cl ₂ Sn)/AC-250	250	313.1	181.7	131.4	0.12	0.06	0.18
(SnCl ₄ +C ₁₆ H ₃₄ Cl ₂ Sn)/AC-300	300	378.5	338.4	40.1	0.29	0.02	0.31

292

293

294

295

296

297

298

299

300

301

302

303

304

305

306

307

308

309 **Table 3.** Textural properties of (SnCl₄+C₁₆H₃₄Cl₂Sn+C₂N₄H₄)/AC calcined at different
 310 temperatures. The molar ratio of SnCl₄, C₁₆H₃₄Cl₂Sn, and C₂N₄H₄ was 1.6:1.0:4.9.

311

Sample	Calcinations Temperature (°C)	S _{BET} (m ² /g) ^a	S _{mic} (m ² /g) ^b	S _{ext} (m ³ /g) ^c	V _{mic} (m ³ /g)	V _{meso} (m ³ /g) ^d	V _{total} (m ³ /g) ^e
(SnCl ₄ +C ₁₆ H ₃₄ Cl ₂ Sn+C ₂ N ₄ H ₄)/AC-150	150	173.3	135.0	38.3	0.07	0.05	0.11
(SnCl ₄ +C ₁₆ H ₃₄ Cl ₂ Sn+C ₂ N ₄ H ₄)/AC-200	200	340.5	287.8	52.7	0.12	0.05	0.17
(SnCl ₄ +C ₁₆ H ₃₄ Cl ₂ Sn+C ₂ N ₄ H ₄)/AC-250	250	440.9	372.5	68.4	0.15	0.08	0.23
(SnCl ₄ +C ₁₆ H ₃₄ Cl ₂ Sn+C ₂ N ₄ H ₄)/AC-300	300	567.6	494.3	73.3	0.21	0.06	0.27
(SnCl ₄ +C ₁₆ H ₃₄ Cl ₂ Sn+C ₂ N ₄ H ₄)/AC-350	350	298.9	257.8	47.1	0.11	0.05	0.16
(SnCl ₄ +C ₁₆ H ₃₄ Cl ₂ Sn+C ₂ N ₄ H ₄)/AC-400	400	233.0	160.8	72.2	0.11	0.04	0.15
(SnCl ₄ +C ₁₆ H ₃₄ Cl ₂ Sn+C ₂ N ₄ H ₄)/AC-450	450	314.5	179.7	134.8	0.11	0.08	0.19
(SnCl ₄ +C ₁₆ H ₃₄ Cl ₂ Sn+C ₂ N ₄ H ₄)/AC-500	500	463.8	400.7	63.1	0.17	0.06	0.23
(SnCl ₄ +C ₁₆ H ₃₄ Cl ₂ Sn)/AC-400	400	374.0	300.6	73.4	0.26	0.03	0.29
HgCl ₂ /AC	200	571.0	479.6	91.4	0.20	0.09	0.29

312

313

314

315

316

317

318

319

320

321

322

323

324 **Table 4.** Mass percent of tin in the samples as detected by SEM-EDS.

Sample	Sn wt%
fresh- $C_{16}H_{34}Cl_2Sn+SnCl_4$ /AC	8.94
used- $(C_{16}H_{34}Cl_2Sn+SnCl_4)$ /AC	2.93
fresh- $(C_{16}H_{34}Cl_2Sn+SnCl_4+C_2N_4H_4)$ /AC	7.16
used- $(C_{16}H_{34}Cl_2Sn+SnCl_4+C_2N_4H_4)$ /AC	5.06

325

326

327

328

329

330

331

332

333

334

335

336

337

338

339

340

341

342

343

344

Figures

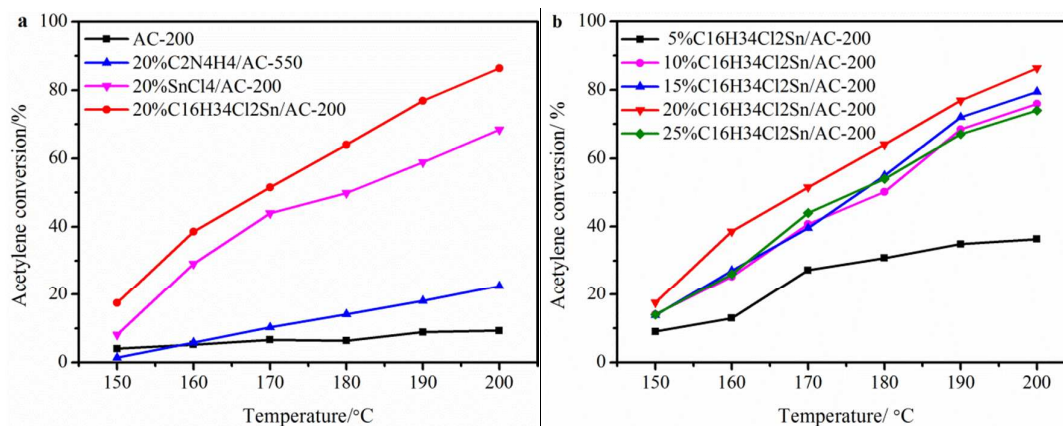
345

346

347 **Fig. 1** (a) Conversion of acetylene for the different catalysts. (b) Catalytic activity of the

348 catalysts containing different amounts of dioctyldichlorotin.

349



350

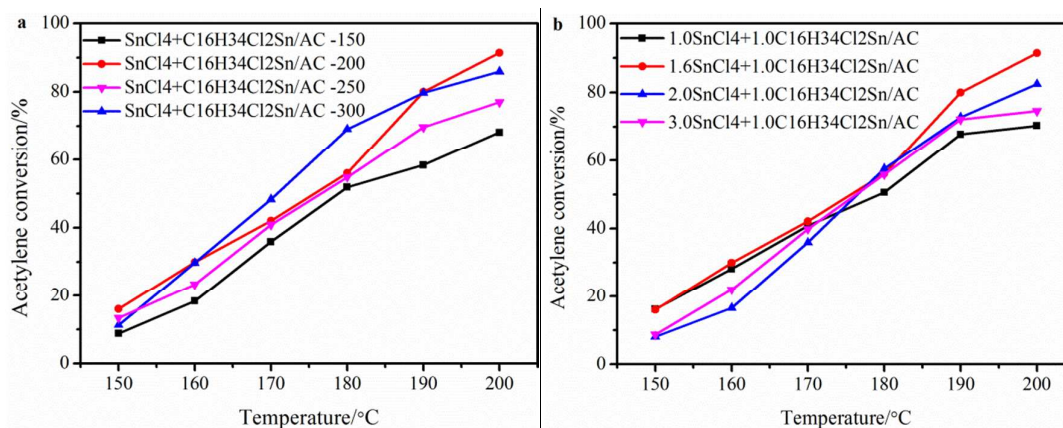
351

352 **Fig. 2** Conversion of acetylene for (SnCl₄+C₁₆H₃₄Cl₂Sn)/AC at (a) different

353 calcination temperatures, and (b) various mole ratio of tin compounds.

354 (1.0SnCl₄+1.0C₁₆H₃₄Cl₂Sn)/AC-150 with a SnCl₄:C₁₆H₃₄Cl₂Sn molar ratio of 1.0:1.0. The

355 calcination temperature was 150 °C.



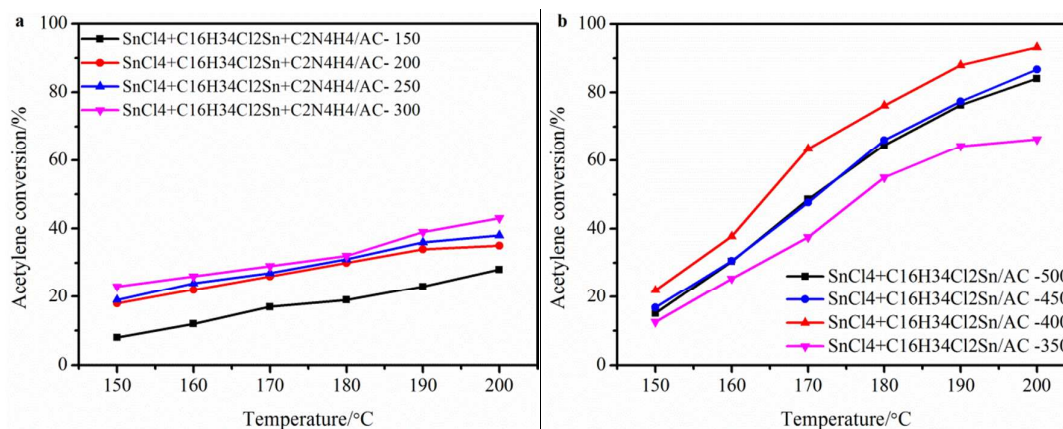
356

357

358 **Fig. 3** Conversion of acetylene for (SnCl₄+C₁₆H₃₄Cl₂Sn+C₂N₄H₄)/AC calcined at different

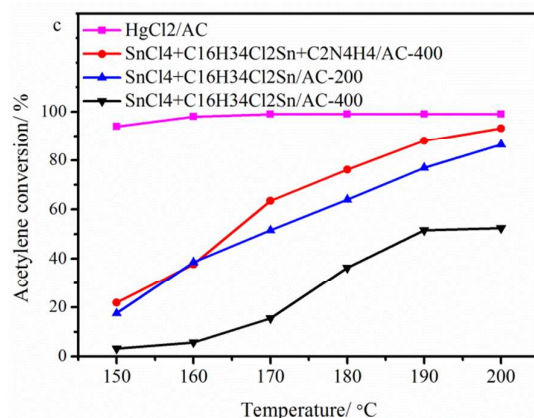
359 temperatures.

360



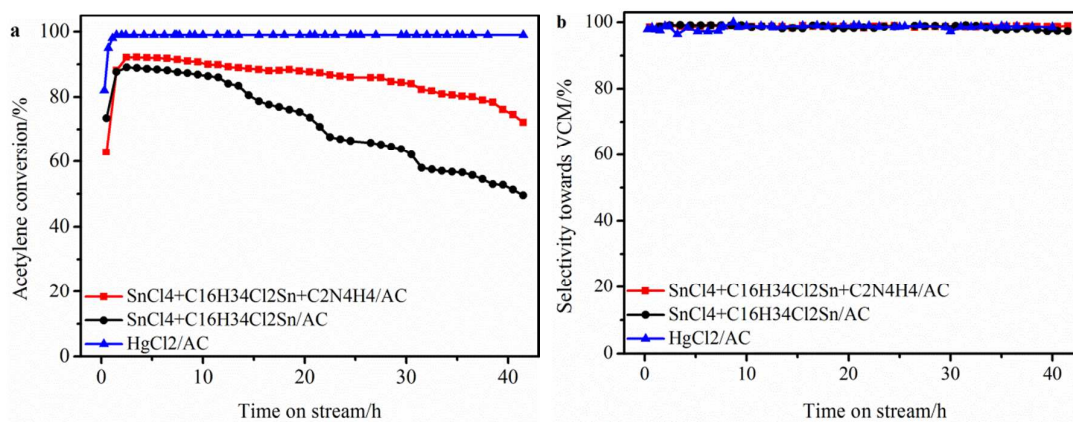
361

362



363

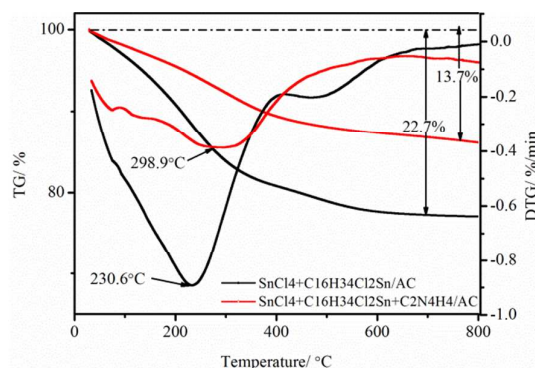
364 **Fig. 4** Catalytic performance of HgCl₂/AC, (SnCl₄+C₁₆H₃₄Cl₂Sn)/AC and
 365 (SnCl₄+C₁₆H₃₄Cl₂Sn+C₂N₄H₄). (a) conversion of acetylene; (b) selectivity towards vinyl
 366 chloride monomer (VCM).



367

368

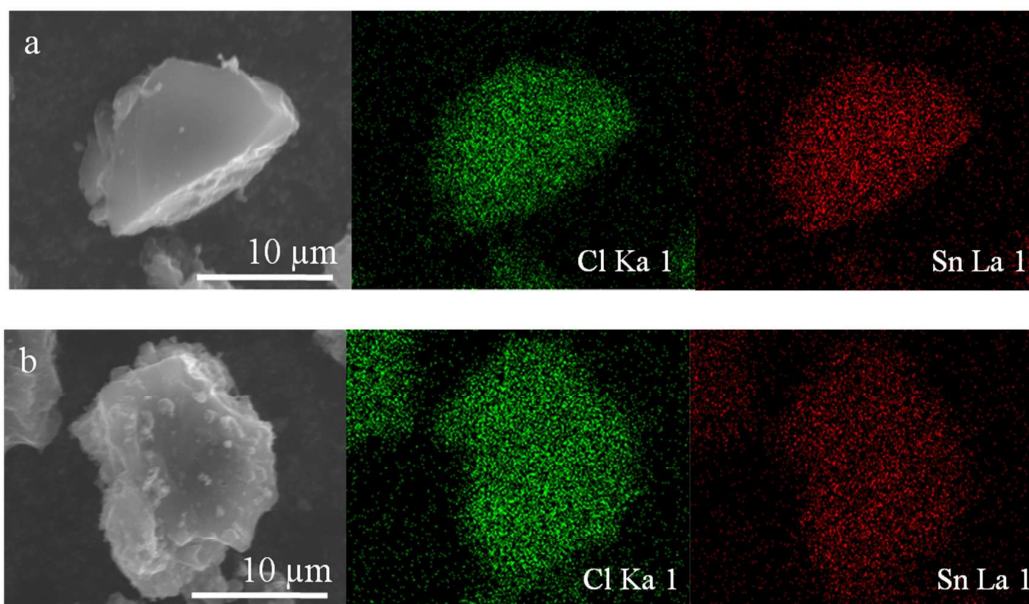
369 **Fig. 5** TGA and DTG curves of the $(\text{SnCl}_4+\text{C}_{16}\text{H}_{34}\text{Cl}_2\text{Sn}+\text{C}_2\text{N}_4\text{H}_4)/\text{AC}$ and
 370 $(\text{SnCl}_4+\text{C}_{16}\text{H}_{34}\text{Cl}_2\text{Sn})/\text{AC}$ catalysts.



371

372

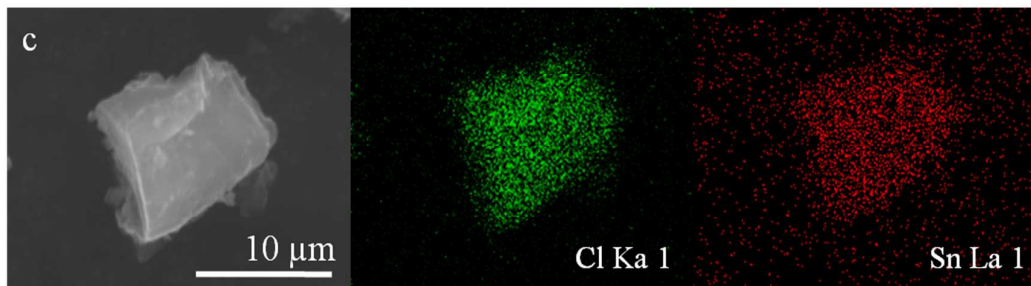
373 **Fig. 6** SEM micrographs and tin and chloride EDS elemental maps of the fresh samples: (a)
 374 fresh- $(\text{SnCl}_4+\text{C}_{16}\text{H}_{34}\text{Cl}_2\text{Sn})/\text{AC}$ and (c) fresh- $(\text{SnCl}_4+\text{C}_{16}\text{H}_{34}\text{Cl}_2\text{Sn}+\text{C}_2\text{N}_4\text{H}_4)/\text{AC}$ and after 36
 375 h of reaction: (b) used- $(\text{SnCl}_4+\text{C}_{16}\text{H}_{34}\text{Cl}_2\text{Sn})/\text{AC}$ and (d) used-
 376 $(\text{SnCl}_4+\text{C}_{16}\text{H}_{34}\text{Cl}_2\text{Sn}+\text{C}_2\text{N}_4\text{H}_4)/\text{AC}$.



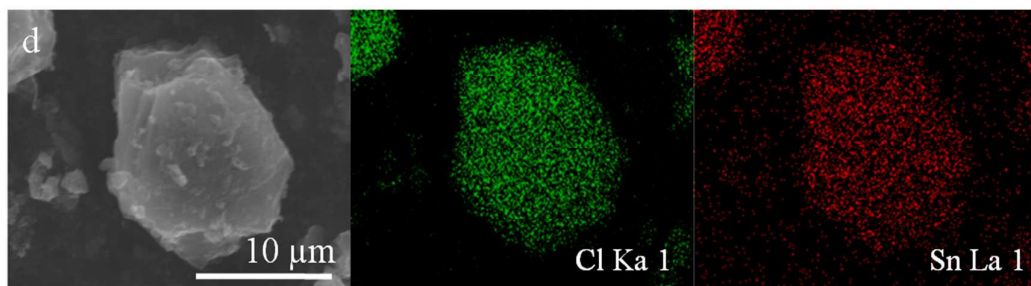
377

378

379



380



381

382